Iron silicides formation on Si (100) and (111) surfaces through theoretical modeling of sputtering and annealing

I.V. Chepkasov [a,b], V.S. Baidyshev [a], E.V. Sukhanova [c,e], M.A. Visotin [d], P. Süle [f], Z.I. Popov [b,e]

[a] *Katanov Khakas State University, 90 Lenin pr., 655017 Abakan, Russia*
[b] *National University of Science and Technology MISiS, 4 Leninskiy pr., 119049 Moscow, Russia*
[c] *Moscow Institute of Physics and Technology (National Research University), 9 Institutskiy per., Dolgoprudny, Moscow Region 141701, Russian Federation*
[d] *Kirensky Institute of Physics, 50/38 Akademgorodok, Krasnoyarsk 660036, Russian*
[e] *Emanuel Institute of Biochemical Physics RAS, Moscow 199339, Russia*
[f] *EK-MFA, Dept. of Nanostructures, Budapest, Hungary*

ARTICLE INFO

ABSTRACT

The iron silicides formation during epitaxial films grown process on the (100) and (111) silicon surfaces were investigated using molecular dynamics (MD). The iron and silicon atom deposition rate and silicon substrate temperature influence on the formed iron silicides structure and stoichiometric composition were studied in detail. During the growth of iron silicides crystal structure significant diffusion of the substrate atoms into the forming BCC core occurs, this intensifies with the substrate temperature increase, and the ratio of substrate atoms inside the Fe_3Si phase reaches nearly 12%. The BCC structure formation is less active on the (100) surface, and at the temperatures as low as 26 °C and 300 °C the iron silicide crystal phase does not form at all. However, with the temperature increase or the deposition rate decrease, the crystal structure formation processes occur more active in both cases of (100) and (111) surfaces. Thus, the effect of the deposition rate decrease is identical to the temperature growth. It was shown that the formation of the structured B2 phase of iron silicide in buffer layer between the film and the substrate leads to the inhibition of the mutual diffusion of iron and silicon atoms.

1. Introduction

Investigations of variable composition epitaxial thin films formation on silicon substrates attract much interest due to especially pronounced interconnection of optical, electrical, and magnetic properties in materials of this class [1–4], which can be controlled during synthesis. Epitaxial thin films of ferromagnetic $Fe_{1-x}Si_x$ are of particular interest because of possible application in silicon based spintronics [5–7]. However, during the initial stages of iron deposition on monocrystalline silicon substrates several phases of non-magnetic silicides are uncontrollably formed even at room temperature [8]. These compounds negatively affect the spin polarization and can even completely destroy it. Iron-silicon phase diagram displays several iron silicide phases, which can be formed on the silicon surface: Fe_3Si, Fe_5Si_3, ε-FeSi, α-FeSi$_2$, β-FeSi$_2$. Multilayer systems $(Fe/Si)_n$ and $(Fe_3Si/β-FeSi_2)_n$ grown on silicon substrates exhibit such phenomena as interlayer exchange interactions and giant magnetoresistance, which makes these systems very promising candidates for creating highly efficient data storage and functional material for non-volatile memory [9–12]. Much attention is also paid to Fe_5Si_3 ferromagnetic silicide, since it can show a giant magnetoresistance effect (2400%) when implanted into silicon, but is thermodynamically unstable in the bulk at room temperature [13]. Nevertheless, the highest interest is attracted to Fe_3Si silicide [14–19], which is metal-

lic and has a high Curie temperature above 800 K, a relatively high spin polarization of ~45% [20], and, thus, is a promising material for spintronics [21]. As known, the magnetic properties are determined by the local ordering [22] which can change during the formation of thin films due to various synthesis parameters [23]. Karel et al. [24] had investigated the magnetic and electronic properties of epitaxial off-stoichiometry Fe_xSi_{1-x} (0.5 < x < 1.0) thin films with chemically ordered (B2 and D0$_3$) and disordered BCC phases. It was determined that magnetic moment in the fully disordered BCC structure is higher than for B2 and D03 due to hybridization of Fe-Si. The decreasing of Fe-Si pair number leads to less s–Si and d–Fe hybridization which results in higher overall magnetization [7]. In a random solid solution the probability of Fe-Si pair formation is much less than in the chemically ordered structure. In addition to a chemically disordered BCC structure, the formation of an amorphous phase of a similar stoichiometry is also possible. Recent investigation of amorphous Fe_3Si shows that Si atoms in amorphous phase prefer to bond with Fe and increase of Si neighbor number suppresses the magnetization of Fe. Small number of Si neighbors is beneficial for the enhancement of spin polarization at the Fermi level because of charge transfer from Si to Fe [25].

Due to the fact that even slight deviations in the process of synthesis of the silicide thin films can lead to a change in their properties, special attention is paid to study the formation conditions, composition and properties of the emerging interfaces [26,27]. The factors, which

can affect the processes of iron silicide formation at the initial stages, include substrate orientation, surface condition, temperature regimes, amount of deposited material, and deposition rate [28–31]. In particular, a slight deviation of the substrate temperature may lead to dramatic changes in the resulting structure, and thus the results obtained by different research groups during identical experiments can deviate significantly from each other [32]. Also, the mutual diffusion of atoms between the deposited phase and the substrate can affect the structure of the growing film [33,34], e.g. can lead to formation of pseudomorphic B2-FeSi (with CsCl-type structure) phase buffer layer between Fe_3Si iron silicide and Si substrate [35]. Moreover, in contrast to bulk structures, diffusion at the interface region is more complex and should be explained at an atomic scale. This allows us to make an assumption that the discrepancies in the results of studies of the formation of thin silicide films can be associated with the laws governing the formation of these materials, which requires additional study.

In turn, the use of modern computer simulation techniques, in particular the molecular dynamics (MD) method, and interatomic interaction potentials having ever-growing accuracy in description of metal–semiconductor systems behavior, allows comprehensive studies of iron silicides formation. The molecular dynamics method has been successfully used to simulate the growth processes of various metal [36–39], semiconductor [40–42], and also metal – semiconductor films [43–45] where the influence of the substrate temperature, deposition angle, and surface orientation on the structural properties of the synthesized films were examined in detail. In particular, the MD simulation of the growth of a hydrogenated silicon film on Si (001) substrate were used for studying the influence of the incidence angle of the deposited atoms. It was determined that in case of incidence angles 0°, 15° and 30° the a-Si:H thin film has an atomically smooth surface. The opposite result was observed in the case wherein the incident angle approaches high incidence (60° and 75°), it grows in a columnar or island-like mode and has rough surface [42]. In the MD simulation of copper thin film growth on silicon (001) surface, the influence of silicon substrate temperature on the structure formation in the deposited layer and atomic diffusion in the interface zone was studied [43].

The theoretical modeling of film growth on silicon substrates up to date are mainly aimed at study of single parameter effects. Also, due to the complexity of interatomic interactions description, there were difficulties in large-scale computer simulation of the processes occurring in co-deposition of iron and silicon atoms on silicon substrates leading to formation of iron silicides. Therefore, this work represents a comprehensive theoretical investigation of iron silicide thin film formation aimed at elucidating the thin films growth mechanisms occurring in real MBE experiments. In this work, we mainly focused on the formation of Fe_3Si silicide films, which have promising spin-polarization properties, but the process of its formation has been little studied on the atomic scale.

2. Computational methodology

The presented computer model for investigation of growth processes in iron silicide thin films during sputtering was created to carefully account for the events occurring in experimental setups for epitaxial film growth [46–48]. Modeling of iron and silicon atoms co-deposition on the (111) and (100) silicon substrates was carried out using molecular dynamics methods in GPU-accelerated [49] LAMMPS program package [50]. Verlet algorithm with a time step of t = 0.5 fs was used for numerical integration of equations of motion. The substrate was modeled by a rectangular block of crystalline Si with the sizes of (19.43 × 43.14 × 43.14) Å and (19.41 × 44.23 × 45.18) Å for (100) and (111) substrates, respectively. Periodic boundary conditions were applied along *y* and *z* axes, while the atoms were sputtered at an angle to the *x* axis.

Substrate atoms were divided into three groups (Fig. 1). The first group (*freezed*) included atoms from the lower two atomic planes and the velocities of these atoms were zeroed at each time step during
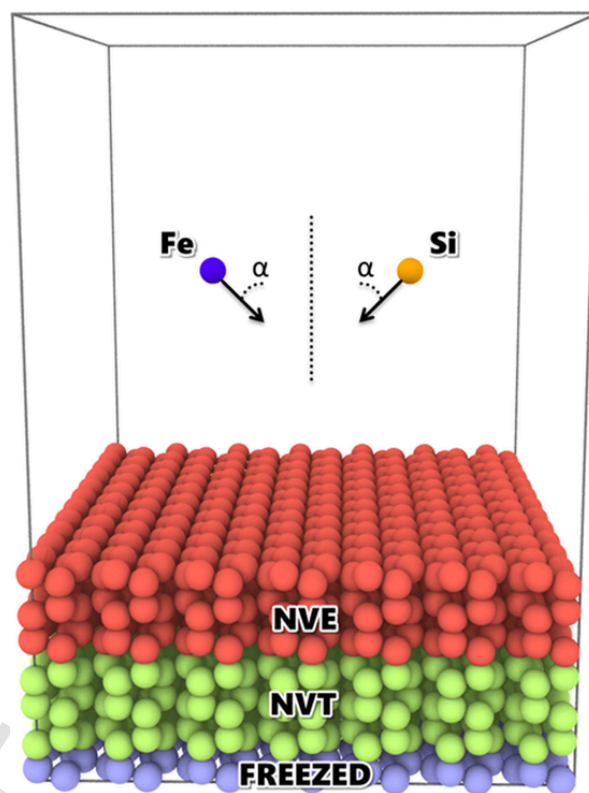

Fig. 1. A scheme of the model for iron and silicon atoms co-deposition.

the simulation in order to avoid substrate displacement and deformation. The second group of atoms (*NVT*) consisted of 6 atomic planes and represented a "thermalization layer" with a Nose-Hoover thermostat (NVT) controlling the temperature. The main purpose of this layer was to maintain a constant substrate temperature while absorbing kinetic energy of the incident atoms and the heat released during the formation of bonds. The third group of atoms (*NVE*) included the upper part of the substrate (6 atomic planes and the deposited atoms). During the modeling this group of atoms was not subjected to temperature control. This approach appears to be a physically adequate way to deal with rather large amounts of energy which are locally released during deposition process as a result of the of bonds formation between the atoms, which may be an essential aspect of the deposited structure formation.

Before the deposition process the substrate was relaxed at a given temperature: first, the NPT thermostat-barostat dynamics for 0.5 ns was carried out to relieve internal stress, followed by 0.5 ns of MD with NVT-thermostat alone. The deposited atoms were being added during simulation to the system at a position of 35 Å above the substrate's upper plane. The angle α between the deposition direction, i.e. initial velocities of deposited atoms and the normal to the substrate's surface was 14°. The magnitude of deposited atom velocity was selected in accordance with the thermal velocity at a temperature T = 1000 K. For the reference system the time intervals between the successive depositions of atoms, Δτ, were 9 ps and 27 ps for iron and silicon atoms, respectively, which corresponds to the Fe:Si stoichiometry of 3:1. The chosen deposition rates allow complete damping of local temperature fluctuations caused by atom collisions with the substrate before the next atom appearance. Also, other deposition rates with Δτ = 45 ps, Δτ = 90 ps for Fe and Δτ = 135 ps, Δτ = 270 ps for Si atoms were considered. The average temperature of the growing film layer differed from the NVT layer temperature by not more than 10°.

The results of calculations were postprocessed and visualized using the Open Visualization Tool (OVITO) [51]. The CNA (Common Neighbor Analysis) method was used to study the lattice structures in

grown silicides with the cutoff radius of 3.475 Å which corresponds to the middle value between the second and the third coordination spheres in bulk Fe_3Si. Additional analysis of emerging phases was made by simulating selected area electron diffraction (SAED) patterns in LAMMPS [52]. The method created by Coleman allows building SAED patterns without *a priori* knowledge of the studied unit cell. The SAED patterns were visualized by plotting logarithm-scaled diffraction intensities in reciprocal space using the VisIt program [53].

For description of Fe-Si interactions in the MD simulations a specific bond order potential (BOP) was used for which has been developed recently [54]. This Albe-Erhart-type BOP was fitted to various experimental and *ab initio* DFT results for Fe-Si systems using the parametrization procedure implemented in the PONTIFIX code by P. Erhart [55]. The BOP potential was parametrized using an extended training set of various structures (dimer, B1 (NaCl), B2 (CsCl), B3 (ZnS), B20 (ε-FeSi), Fe_3Si (DO$_3$) phases for FeSi), which is a good pre-requisite for applicability in MD simulation of thin film growth. The Fe-Si interaction parameters set BOP-IIb from [54] was used, because of its more stable behavior in annealing simulations and more accurate description of under-coordinated atoms, e.g. Fe-Si dimer. Pure Si-Si interaction parameters were fitted simultaneously with BOP-IIb parameters, while the pure Fe-Fe parameter set was taken from [56].

All quantum-chemical calculations were performed within the framework of density functional theory (DFT) [57,58] implemented in VASP program package [59–61]. The Perdew, Burke and Ernzerhof (PBE) exchange-correlation functional was used [62]. The projector-augmented wave (PAW) method based pseudopotential was applied in plane wave basis with the energy cutoff of 300 eV. The Brillouin zone sampling was made by the Monkhorst-Pack scheme with the smallest allowed spacing between k-points of 0.2 Å^{-1}. The structural relaxation was performed until the difference in energy between two steps was less than 0.01 eV with the preservation of the cubic cell shape.

3. Results and discussion

3.1. Growing of iron silicides

In order to study the effect of substrate temperature on the structure of growing iron silicide films we simulated the Fe and Si atoms co-deposition on a silicon substrate at different temperatures (26 °C, 300 °C, and 1200 °C). The role of the deposition rate was examined using three different time intervals between collisions of atoms and the substrate: 9 ps, 45 ps, and 90 ps for iron atoms, the corresponding intervals for silicon atoms were three times longer. The results of structure and composition analysis of deposited iron silicide films on (100) and (111) silicon substrates are presented in Tables 1 and 2.

The structures of Fe_3Si films obtained at different synthesis parameters, including the interval between two Fe atoms depositions $\Delta\tau$ and the temperature T, were characterized by: the total number of atoms in the BCC region N(BCC), the number of deposited Si atoms in the BCC region N(Si_d), the number of Si atoms in the BCC region, which have diffused from the substrate N(Si_s), the number of deposited Fe atoms in the BCC region N(Fe), the number of silicon (N(Si_n)) and iron (N(Fe_n)) atoms having 8 neighbors of other atoms types in the BCC structure within the first coordination sphere (2.65 Å), which should be present in case of ideal Fe_3Si phase.

Basing on the result of computer modeling it can be concluded that the silicon substrate orientation have a great influence on the structure of deposited iron silicide films. Tables 1 and 2 show that the structure formation on Si(100) is less active than on Si(111) surface, and at low temperatures of 26 °C and 300 °C the crystal lattice does not form at all. However, with the temperature increase and with the deposition rate decrease the processes of crystal structure formation become more active for both Si(100) and Si(111) substrates. Moreover, the deposition rate reduction can lead to the same result as the substrate temperature increase within the range considered here. In particular, in case of deposition on Si(111) with $\Delta\tau$(Fe) = 9 ps the increase of substrate temperature from 26 °C to 300 °C leads to the increase in the number

Table 1
The results of structure and composition analysis of the silicide thin films grown on Si(100).

Δτ,ps	T, °C	N(BCC), at.	N(Si_s), at.	N(Si_d), at.	N (Fe), at.	N (Si_n), at.	N(Fe_n), at.
9 ps	26 °C	0	0	0	0	0	0
9 ps	26 °C	0	0	0	0	0	0
9 ps	300 °C	0	0	0	0	0	0
9 ps	300 °C	0	0	0	0	0	0
9 ps	1200 °C	3003(55.8%)	232(7.7%)	701(23.3%)	2070(68.9%)	898(96.24%)	551(26.61%)
9 ps	1200 °C	2347(43.6%)	276(11.8%)	590(25.1%)	1481(63.1%)	817(94.34%)	442(29.84%)
45 ps	26 °C	0	0	0	0	0	0
45 ps	300 °C	766(14.3%)	22(2.9%)	213(27.8%)	531(69.3%)	147(62.5%)	3(0.5%)
90 ps	26 °C	0	0	0	0	0	0
90 ps	300 °C	1604(32.8%)	78(4.9%)	424(26.4%)	1102(68.7%)	305(60.75%)	16(1.45%)

Table 2
The results of structure and composition analysis of the silicide thin films grown on Si(111).

Δτ,ps	T,°C	N(BCC), at.	N(Si_s), at.	N(Si_d), at.	N(Fe), at.	N(Si_n), at.	N(Fe_n),at.
9 ps	26 °C	337(5.9%)	2(0.6%)	101(30%)	234(69.4%)	71(68.93%)	6(2.5%)
9 ps	26 °C	994(17.4%)	7(0.7%)	261(26.3%)	726(73%)	171(63.80%)	11(1.5%)
9 ps	300 °C	1924(34%)	36(1.9%)	510(26.5%)	1378(71.6%)	348(63.73%)	15(1.08%)
9 ps	300 °C	1959(34.6%)	45(2.3%)	510(26%)	1404(71.1%)	382(68.82%)	13(0.92%)
45 ps	26 °C	159(2.8%)	4(2.5%)	45(28.3%)	110(69.2%)	32(65.30%)	3(2.72%)
45 ps	26 °C	720(12.6%)	2(0.3%)	189(26.2%)	529(73.5%)	114(59.68%)	5(0.94%)
45 ps	300 °C	2667(46.8%)	77(2.9%)	693(26%)	1897(71.1%)	486(63.11%)	30(1.8%)
45 ps	300 °C	2298(40.3%)	58(2.5%)	610(26.5%)	1630(70.9%)	445(66.61%)	25(1.5%)
90 ps	26 °C	2185(38.3%)	22(1.1%)	578(26.5%)	1584(72.5%)	320(53.33%)	7(0.4%)
90 ps	300 °C	2161(37.9%)	100(4.6%)	566(26.2%)	1495(69.2%)	449(67.41%)	36(2.4%)

of atoms with BCC structure by 17–28%. In the structures obtained at the same substrate temperature of 300 °C the increase of deposition time interval $\Delta\tau$ (Fe) from 9 ps to 45 ps results in 6–12% increase in N(bcc). This effect can be explained by the fact that lower deposition rates give more time for the atom to find the most energetically favorable position during chaotic movement on the surface before being blocked by new atoms. On the other hand, higher temperatures increase the rates of atom jumping between the sorption positions and promote overcoming the barriers of structural transformations.

The influence of incidence angle α on the structure of growing film was also tested by additional simulations with α = 45° at different temperatures (T = 300 or 1200 °C) and different deposition rates ($\Delta\tau$(Fe) = 9 or 90 ps). The results were similar to the corresponding simulations with α = 14°, so the influence of α < 45° should be assumed negligible compared to the other factors. However, more oblique deposition may lead to change of the growth mode [42].

Typical examples of Fe_3Si iron silicide structures obtained on Si(100) and Si(111) substrates are shown in Figs. 2 and 3, along with the results of CNA structural analysis and the corresponding simulated SAED patterns for the full structure and for found BCC clusters only. It was found that the grown BCC lattice also contains silicon atoms which were originally a part of the substrate and diffused during the simulation into the formed silicide film (shown as Si(s) in Figs. 2 and 3). The number of such atoms was different for Si(100) and Si(111) surfaces: not more than 11.8% for Si(100) and less than 4.6% for Si(111). It is clearly noticeable that the number of such atoms and the diffusion distance increases with rise of synthesis temperature.

The crystallinity of grown silicide films can be also assessed by analyzing the calculated SAED patterns for the whole structure, including the substrate, and SAED patterns of diffraction only from the BCC clusters. The presence of high-intensity thick diffuse rings in the full-structure SAED patterns for the deposition at low temperatures con-
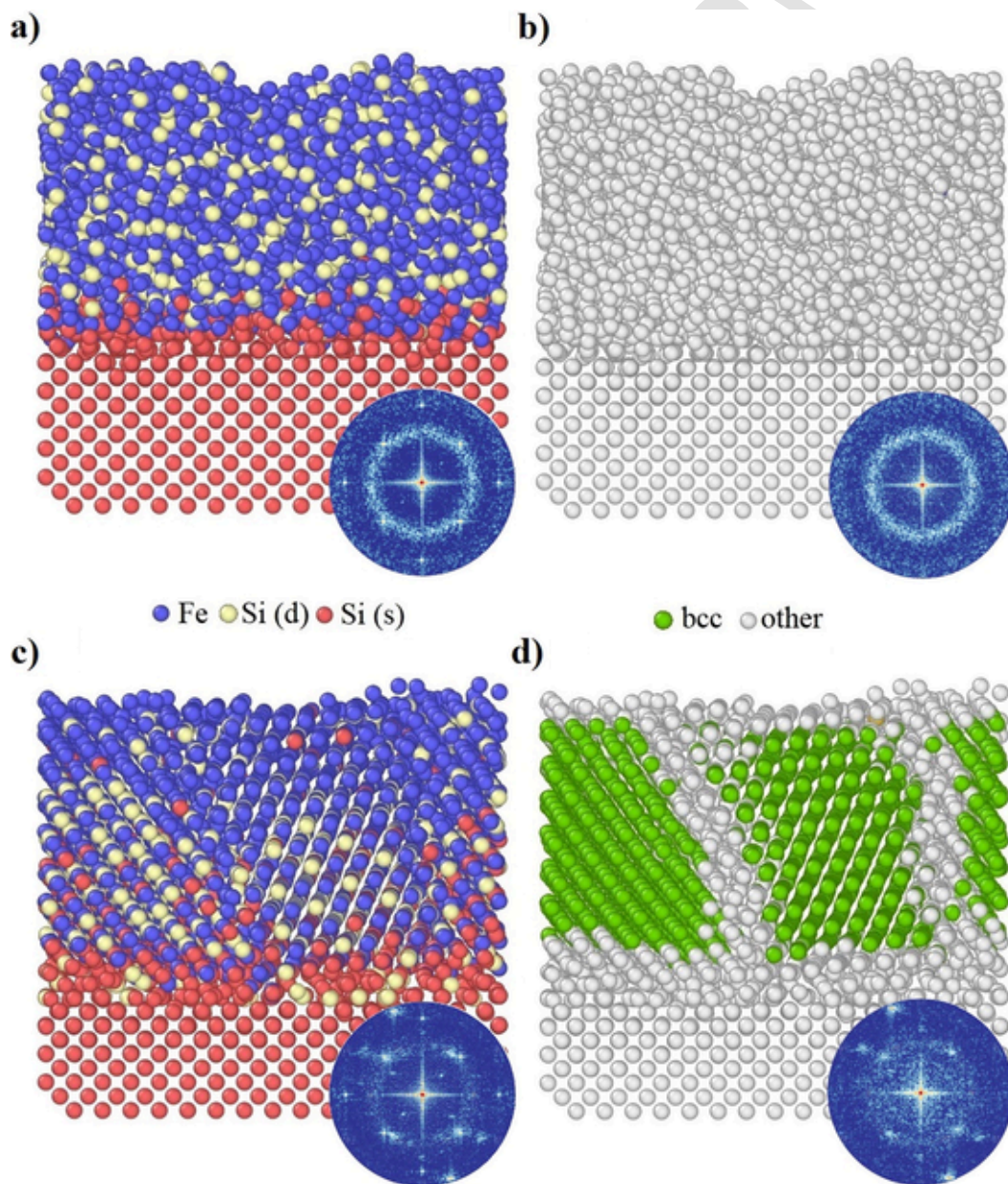

Fig. 2. The atomic structures of Fe_3Si films grown on Si(100) at T = 26 °C, $\Delta\tau$(Fe) = 9 ps (a, b) and T = 1200 °C, $\Delta\tau$(Fe) = 9 ps, (c, d). The overall view of the structures are to the left (a, c), the *CNA* analyzed structures are to the right (b, d). Si(s) are silicon atoms originated from the substrate, Si(d) are the deposited silicon atoms. The insets in the bottom of the pictures are the calculated SAED patterns for the full structure (left) and for the BCC cluster (right); the zone axis is along Si[100].
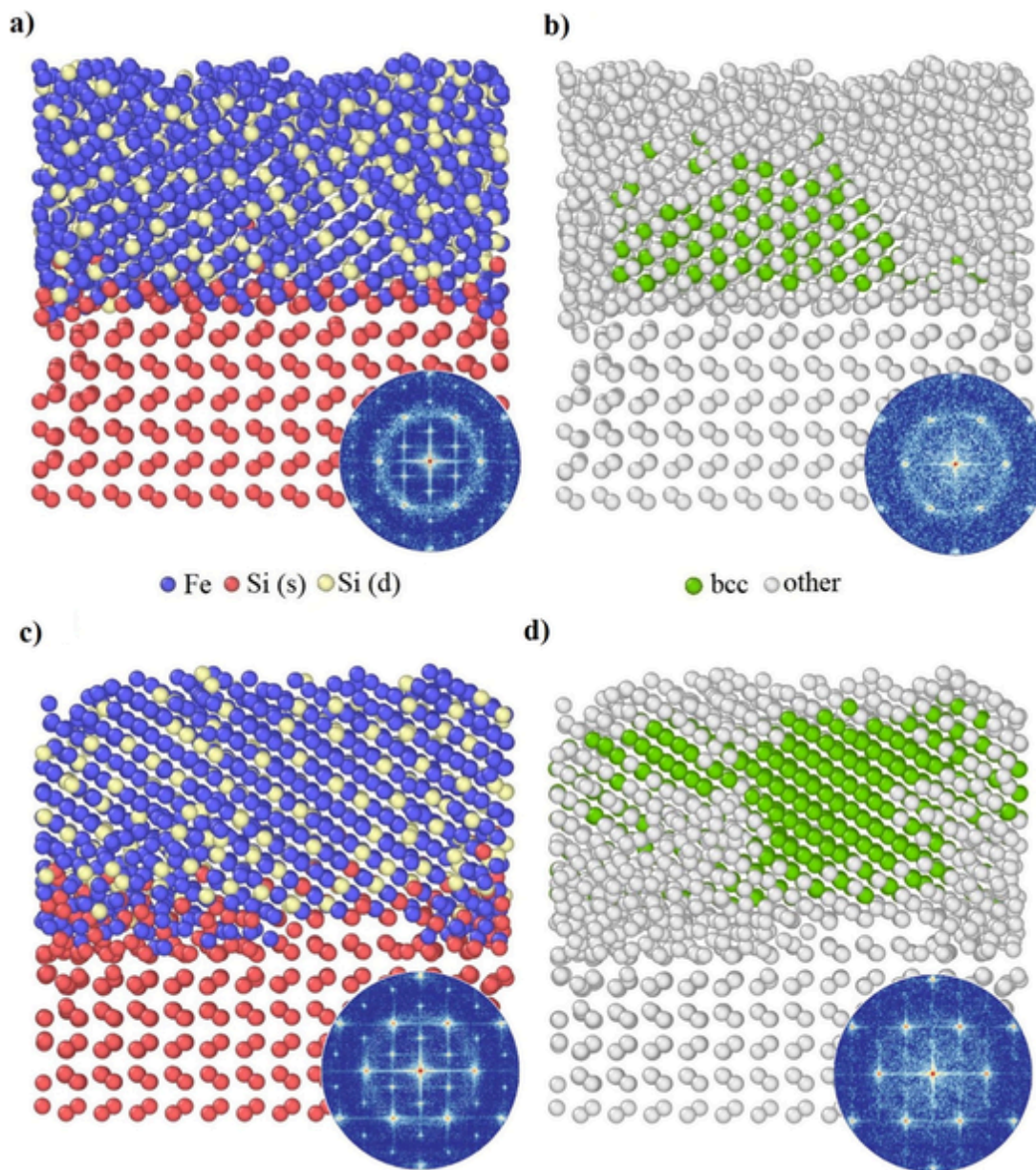
Fig. 3. The atomic structures of Fe_3Si films grown on Si(111) at T = 26 °C, $\Delta\tau$(Fe) = 9 ps (a, b) and T = 300 °C, $\Delta\tau$(Fe) = 9 ps (c, d). The overall view of the structures are to the left (a, c), the *CNA* analysed structures are to the right (b, d). Si(s) are silicon atoms originated from the substrate, Si(d) are the deposited silicon atoms. The insets in the bottom of the pictures are the calculated SAED patterns for the full structure (left) and for the BCC cluster (right); the zone axis is along Si[111].

firms growth of amorphous SiFe films (Figs. 2a-b, 3a-b). On the other hand, the blurriness and intensity of the diffuse rings decreases with the increase of synthesis temperature showing better quality of obtained structures. The diffraction patterns obtained only from the BCC clusters display a 6-fold set of bright spots in the case of growth on the Si(111) substrate, which corresponds to a good epitaxial growth of Fe_3Si with (111) planes oriented parallel to the substrate surface. For the films grown on Si(100) surface at T = 1200 °C, with $\Delta\tau$(Fe) = 9 ps (Fig. 3c-d), two sets of reflexes can be identified in the SAED patterns from the BCC clusters only, which is an evidence of twinning in the films. Indeed, a closer look at the simulation cell reveals two distinct BCC lattice domains inside the film, thus the obtained structure can be treated as a polycrystalline thin film.

The resulting Fe content in the growing BCC domains varies within 67–74% atomic. Despite the stoichiometry of the deposited layer is close to 3:1 with cubic lattice, the growing films identified as a disordered alloy with the absence of DO_3 Fe_3Si phase. This can be

clearly seen from the distribution of iron-type neighbor counts within the first and the second coordination spheres around the atoms which is closer to random binomial distribution rather than to discrete distribution in DO_3 Fe_3Si (Fig. S1). In order to investigate the origin of disordering in the BCC structure of iron silicide the formation energies of Fe_3Si with all possible ordering inside the unit cell containing 16 atoms were calculated with BOP potential and within Density Functional Theory approach. As can be seen from Fig. 4 the energy difference between any ordering of Fe_3Si and the DO_3 structure lies in the range from 0.10 to 0.16 eV. Therefore, we suggest that such low values make the local stoichiometric disordering possible on condition of inhomogeneous grow and temperature gradient near the substrate. It is also worth noting that the energy difference between Fe_3Si with DO_3 structure and the others obtained with the BOP interatomic potential and with DFT agree well, which additionally validates the applicability of the chosen BOP potential.
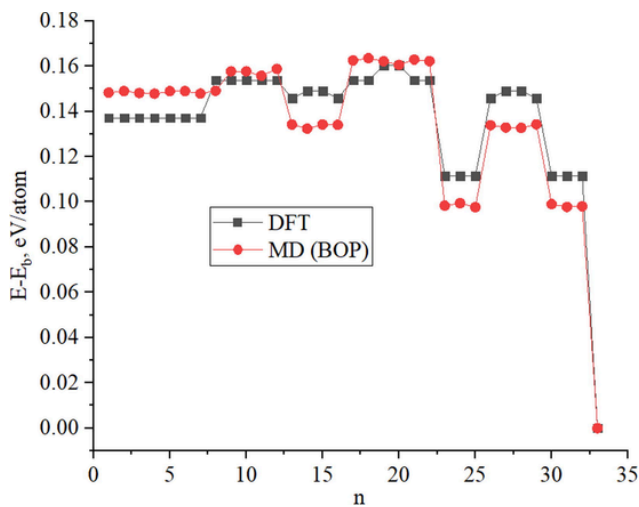
Fig. 4. Energy difference between any Fe_3Si (E) structures and Fe_3Si with $D0_3$ structure (E_b) in the unit cell with 16 atoms. n - options for the arrangement of atoms from a Fe_3Si cell.

3.2. Annealing of iron silicides

In addition, simulation of annealing was carried out for amorphous Fe_3Si films, which had failed to form crystalline structure during the deposition. The annealing lasted for 20 ns (100 million steps) at a temperature of 1200 K. To assure stability of the substrate the two lower silicon layers were fixed (freezed) at all simulation stages. The initial structure for annealing was taken from the MD simulation of deposition on Si(100) at the following parameters: T = 26 °C, $\Delta\tau(Fe) = 9$ ps (Fig. 2b). The intermediate time snapshots of the structure during the annealing are shown in Fig. 5a, b, c. The results of CNA analysis for intermediate structures are presented in Fig. 5d, e, f. It can be seen that during the annealing process the deposited amorphous silicide film undergoes gradual ordering resulting in a single BCC crystal.

It is worth noting that the Fe and Si atom interdiffusion processes appear to be terminated with the onset of BCC phase formation in the annealed Fe_3Si silicide film. The diffusion of Fe atoms during the annealing can be seen as a change in stoichiometry and the distributions of Si and Fe atoms along the x axis at the beginning and at the end of annealing (Fig. 5g, h). It was previously shown in the study of Fe_3Si on Si (111)[63] that the temperature dependence of static displacement for Fe atoms is bigger than for Si atoms, which agrees well with our data. A comparison of Fig. 5g and h shows the graph of iron atom spatial distribution is shifted by 5 Å toward the silicon substrate without changing the slope, while the graph of silicon crystal atoms spatial distribution is shifted by 5 Å toward the silicide film with a significant change in the slope angle. An analysis of defect formation enthalpies and migration barriers in the Fe_3Si structure using DFT calculations demonstrated the asymmetric character of iron and silicon atoms diffusion in the structure [64].

Due to the asymmetric nature of interdiffusion, inside the formed diffusion layer in the range from 10 to 25 Å (Fig. 5h) the ratio of Fe atoms to Si differs from the stoichiometry of Fe_3Si. This behavior was also observed during step-by-step vacuum annealing at temperatures of 350 °C, 450 °C, and 550 °C of Fe_3Si silicide films on Si [65]. In particular, it was shown that annealing at temperature of 350 °C causes an increase in the film thickness by ~19%, which is associated with a change in the lattice parameters caused by diffusion of iron atoms into the silicon substrate and the formation of a diffusion layer of silicide. Upon reaching an annealing temperature of 450 °C, the formation of a polycrystalline ε-FeSi sublayer was observed with the subsequent for-

mation of a polycrystalline film containing FeSi, Fe_5Si_3 and $FeSi_2$ phases after annealing at 550 °C. It should be noted that the thickness of the diffusion layer in the structures studied experimentally reaches dozens of nanometers, which is much larger than in our model. In order to investigate the influence of ordered BCC phase formation on mutual diffusion we proposed a following approach, which implies insertion of a B2 BCC layer of FeSi with 1:1 atomic ratio of Fe:Si basing on experimental data from [66,67] between the deposited amorphous phase and the silicon substrate instead of the diffusion layer, with further annealing of the whole structure at a temperature from 300 to 1200 K for 10 ns. As a result of simulation, it was shown that the inserted BCC FeSi layer not only prevented the mutual diffusion of iron and silicon atoms, but also initiated the BCC structure nucleation inside the amorphous Fe_3Si layer (Fig. S2d). Thus, the simulation revealed the effect of the nuclei structure formation on the inhibition of mutual diffusion processes.

4. Conclusions

A proposed methodology for theoretical modeling of bicomponent compound deposition was applied for iron silicides growing procedure simulation. Iron silicide film deposition on silicon substrates of different orientations was simulated and the influence of such parameters as the type of substrate surface (111 and 100), substrate temperature (26 °C, 300 °C, and 1200 °C), and atom deposition rate (3 iron and 1 silicon atoms each 27 ps, 135 ps and 270 ps) on the formed silicide film structure was determined. It was shown that formation of the BCC structure of deposited layer with Fe_3Si stoichiometry is more preferable on Si(111) surface even at low temperatures. The chemical disordering in the BCC structure of iron silicides can be attributed to the proximity of the energies of the disordered structure and ideal $D0_3$ structure Fe_3Si calculated by DFT and by the bond-order-potentials (from 0.1 to 0.16 eV/atom). It was demonstrated that the formation of B2 ordered cubic structure in the interface during annealing of amorphous Fe_3Si film prevents iron and silicon mutual diffusion.

CRediT authorship contribution statement

I.V. Chepkasov: Data curation, Visualization, Investigation, Writing - original draft. **V.S. Baidyshev:** Investigation, Software. **E.V. Sukhanova:** Data curation. **M.A. Visotin:** Software, Writing - review & editing. **P. Süle:** Software. **Z.I. Popov:** Supervision. **:** Methodology, Writing - original draft.

Declaration of Competing Interest

The authors declare that they have no known competing financial interests or personal relationships that could have appeared to influence the work reported in this paper.

Acknowledgements

Appendix A. Supplementary data

Supplementary data to this article can be found online at https://doi.org/10.1016/j.apsusc.2020.146736.
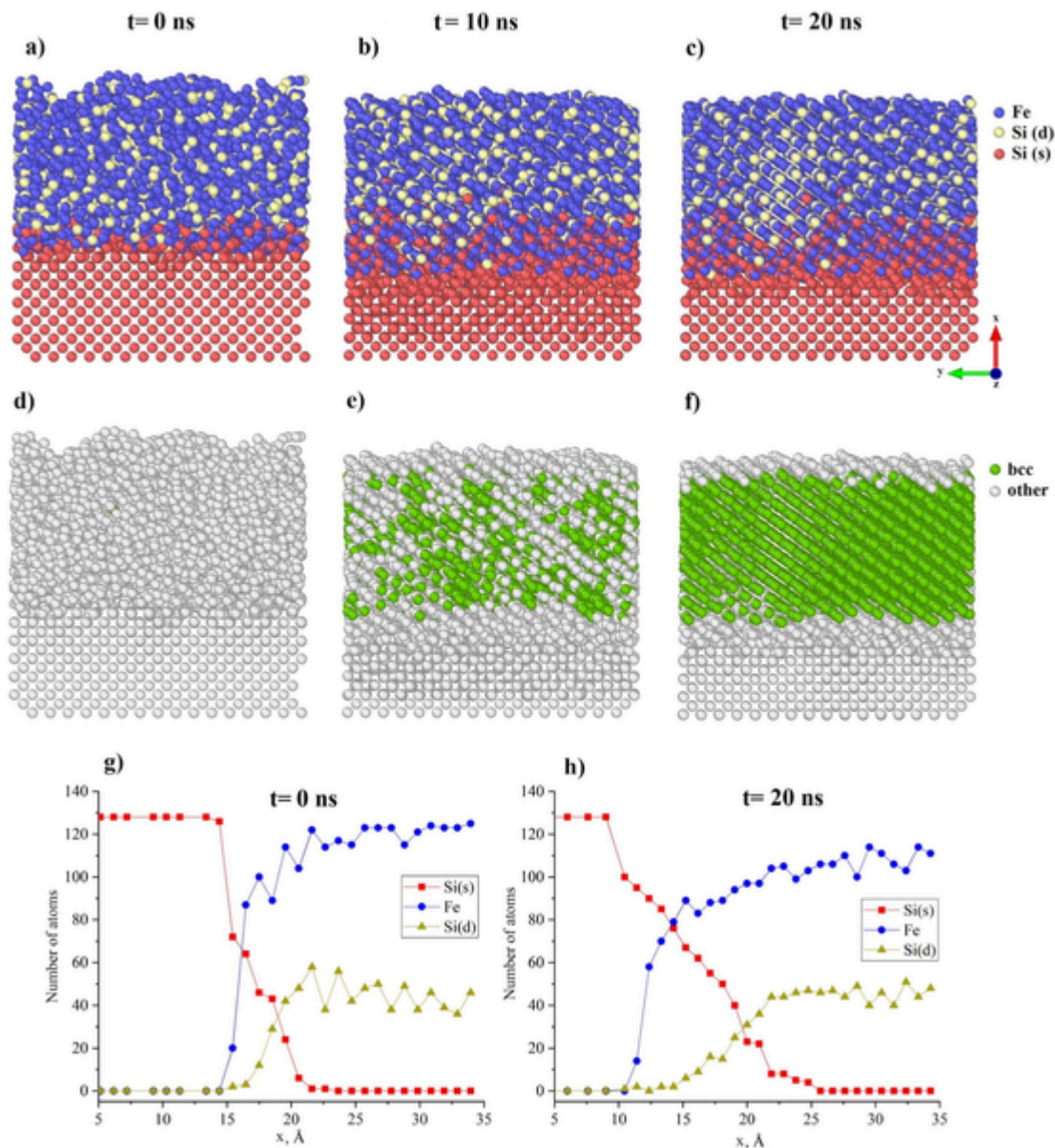
Fig. 5. A–c) Snapshots of the annealing simulation for pre-deposited amorphous Fe₃Si film on Si (100) at T = 1200 K at t = 0, 10 and 20 ns simulation time. d–f) - *CNA* results for the same structures. g, h) Distribution of the number of Fe, Si(s) (substrate silicon atoms), and Si(d) (deposited silicon atoms) along the growth direction.

References

[1] W Liu, P K J Wong, Y Xu, Hybrid spintronic materials: growth, structure and properties, Prog. Mater Sci. 99 (2019) 27–105, doi:10.1016/j.pmatsci.2018.08.001.

[2] R Kawaguchi, T Eguchi, S Suto, Atomistic investigation on the initial stage of growth and interface formation of Fe on H-terminated Si(111)-(1 × 1) surface, Surf. Sci. 686 (2019) 52–57, doi:10.1016/j.susc.2019.04.002.

[3] I Goldfarb, F Cesura, M Dascalu, Magnetic binary silicide nanostructures, Adv. Mater. Weinheim. 30 (2018), doi:10.1002/adma.201800004.

[4] I A Tarasov, Z I Popov, S N Varnakov, M S Molokeev, A S Fedorov, I A Yakovlev, D A Fedorov, S G Ovchinnikov, Optical characteristics of an epitaxial Fe3Si/Si(111) iron silicide film, Jetp Lett. 99 (2014) 565–569, doi:10.1134/S0021364014100105.

[5] S Khmelevskyi, G Kresse, P Mohn, Correlated excited states in the narrow band gap semiconductor FeSi and antiferromagnetic screening of local spin moments, Phys. Rev. B. 98 (2018), doi:10.1103/PhysRevB.98.125205 125205.

[6] J Karel, D S Bouma, J Martinez, Y N Zhang, J A Gifford, J Zhang, G J Zhao, D R Kim, B C Li, Z Y Huang, R Q Wu, T Chen, F Hellman, Enhanced spin polarization of amorphous F ex S i1−x thin films revealed by Andreev reflection spectroscopy, Phys. Rev. Mater. 2 (2018), doi:10.1103/PhysRevMaterials.2.064411 064411.

[7] J Karel, Y N Zhang, C Bordel, K H Stone, T Y Chen, C A Jenkins, D J Smith, J Hu, R Q Wu, S M Heald, J B Kortright, F Hellman, Using structural disorder to enhance the magnetism and spin-polarization in FexSi1 -xthin films for spintronics, Mater. Res. Express. 1 (2014), doi:10.1088/2053-1591/1/2/026102 026102.

[8] S N Varnakov, S V Komogortsev, S G Ovchinnikov, J Bartolomé, J Sesé, Magnetic properties and nonmagnetic phases formation in (Fe/Si)n films, J. Appl. Phys. 104 (2008), doi:10.1063/1.3005973 094703.

[9] L Badía-Romano, J Rubín, C Magén, F Bartolomé, J Sesé, M R Ibarra, J Bartolomé, A Hierro-Rodriguez, J I Martín, J M Alameda, D E Bürgler, S N Varnakov, S V Komogortsev, S G Ovchinnikov, Thermomagnetic behaviour and compositional irreversibility on (Fe/Si)3 multilayer films, J. Magn. Magn. Mater. 364 (2014) 24–33, doi:10.1016/j.jmmm.2014.04.029.

[10] T Yoshitake, T Ogawa, D Nakagauchi, D Hara, M Itakura, N Kuwano, Y Tomokiyo, K Takeda, T Kajiwara, M Ohashi, G Oomi, K Nagayama, Interlayer coupling in ferromagnetic epitaxial Fe3Si/FeSi2 superlattices, Appl. Phys. Lett. 89 (2006), doi:10.1063/1.2410222 253110.

[11] S Hirakawa, T Sonoda, K Sakai, K Takeda, T Yoshitake, Temperature-dependent current-induced magnetization switching in Fe3Si/FeSi2/Fe3Si trilayered films, Jpn. J. Appl. Phys. 50 (2011) 08JD06, doi:10.1143/JJAP.50.08JD06.

[12] P C Srivastava, J K Tripathi, Giant magnetoresistance (GMR) in swift heavy ion irradiated Fe films on c-silicon (Fe/c-Si), J. Phys. D: Appl. Phys. 39 (2006) 1465–1471, doi:10.1088/0022-3727/39/8/001.

[13] K S K Varadwaj, K Seo, J In, P Mohanty, J Park, B Kim, Phase-controlled growth of metastable Fe5Si3 nanowires by a vapor transport method, J. Am. Chem. Soc. 129 (2007) 8594–8599, doi:10.1021/ja071439v.

[14] K Hamaya, K Ueda, Y Kishi, Y Ando, T Sadoh, M Miyao, Epitaxial ferromagnetic Fe3Si/Si(111) structures with high-quality heterointerfaces, Appl. Phys. Lett. 93 (2008), doi:10.1063/1.2996581 132117.

[15] Y Ando, K Hamaya, K Kasahara, Y Kishi, K Ueda, K Sawano, T Sadoh, M Miyao, Electrical injection and detection of spin-polarized electrons in silicon through an Fe3Si/Si Schottky tunnel barrier, Appl. Phys. Lett. 94 (2009), doi:10.1063/1.3130211 182105.

[16] K Hamaya, N Hashimoto, S Oki, S Yamada, M Miyao, T Kimura, Estimation of the spin polarization for Heusler-compound thin films by means of nonlocal spin-valve measurements: comparison of Co2FeSi and Fe3Si, Phys. Rev. B. 85 (2012), doi:10.1103/PhysRevB.85.100404 100404.

[17] S Yamada, J Sagar, S Honda, L Lari, G Takemoto, H Itoh, A Hirohata, K Mibu, M Miyao, K Hamaya, Room-temperature structural ordering of a Heusler compound Fe3Si, Phys. Rev. B. 86 (2012), doi:10.1103/PhysRevB.86.174406 174406.

[18] Y Ando, K Ichiba, S Yamada, E Shikoh, T Shinjo, K Hamaya, M Shiraishi, Giant enhancement of spin pumping efficiency using Fe3Si ferromagnet, Phys. Rev. B. 88 (2013), doi:10.1103/PhysRevB.88.140406 140406.

[19] A S Tarasov, I A Bondarev, M V Rautskii, A V Lukyanenko, I A Tarasov, S N Varnakov, S G Ovchinnikov, N V Volkov, Room temperature spin accumulation effect in boron doped Si created by epitaxial Fe3Si/p-Si schottky contact, J. Synch. Investig. 12 (2018) 633–637, doi:10.1134/S1027451018040171.

[20] A Ionescu, C A F Vaz, T Trypiniotis, C M Gürtler, H García-Miquel, J A C Bland, M E Vickers, R M Dalgliesh, S Langridge, Y Bugoslavsky, Y Miyoshi, L F Cohen, K R A Ziebeck, Structural, magnetic, electronic, and spin transport properties of epitaxialFe3Si/GaAs(001), Phys. Rev. B. 71 (2005), doi:10.1103/PhysRevB.71.094401 094401.

[21] A Hirohata, K Takanashi, Future perspectives for spintronic devices, J. Phys. D: Appl. Phys. 47 (2014), doi:10.1088/0022-3727/47/19/193001 193001.

[22] D L Leslie-Pelecky, R D Rieke, Magnetic properties of nanostructured materials, Chem. Mater. 8 (1996) 1770–1783, doi:10.1021/cm960077f.

[23] M. Iiunua, T. Hiroaki, M. Naoki, Y. Haruki, T. Yoshikazu, Dependence of direct transition energy on growth temperature in β-FeSi epitaxial films, JJAP Conference Proceedings. (2017). https://journals.jsap.jp (accessed January 4, 2020).

[24] J Karel, J Juraszek, J Minar, C Bordel, K H Stone, Y N Zhang, J Hu, R Q Wu, H Ebert, J B Kortright, F Hellman, Effect of chemical order on the magnetic and electronic properties of epitaxial off-stoichiometryFexSi1−x thin films, Phys. Rev. B. 91 (2015), doi:10.1103/PhysRevB.91.144402 144402.

[25] B H Zhang, Z Wang, Y N Zhang, R Q Wu, Effect of structural disordering on magnetic and magneto-optical properties of Fe3Si, Phys. Rev. Materials. 3 (2019), doi:10.1103/PhysRevMaterials.3.095602 095602.

[26] S. Walter, F. Blobner, M. Krause, S.M. ller, K. Heinz, U. Starke, Interface structure and stabilization of metastable B2-FeSi/Si(111) studied with low-energy electron diffraction and density functional theory, J. Phys.: Condens. Matter. 15 (2003) 5207–5221. doi: 10.1088/0953-8984/15/30/303.

[27] S Kim, Y Jung, J Jung Kim, G Byun, S Lee, H Lee, Direct observation of nanometer-scale strain field around CoSi2/Si interface using scanning moiré fringe imaging, Appl. Phys. Lett. 104 (2014) 161610, doi:10.1063/1.4873393.

[28] M V Gomoyunova, D E Malygin, I I Pronin, A S Voronchikhin, D V Vyalikh, S L Molodtsov, Initial stages of iron silicide formation on the Si(100)2×1 surface, Surf. Sci. 601 (2007) 5069–5076, doi:10.1016/j.susc.2007.09.007.

[29] M Dascalu, F Cesura, G Levi, O Diéguez, A Kohn, I Goldfarb, Controlling the supermagnetic response of tetragonal α-FeSi2 nanoislands, Appl. Surf. Sci. 476 (2019) 189–197, doi:10.1016/j.apsusc.2019.01.079.

[30] H Nakano, K Maetani, K Hattori, H Daimon, Variety of iron silicides grown on Si(001) surfaces by solid phase epitaxy: Schematic phase diagram, Surf. Sci. 601 (2007) 5088–5092, doi:10.1016/j.susc.2007.04.234.

[31] I Goldfarb, Y Camus, M Dascalu, F Cesura, R Chalasani, A Kohn, Tuning magnetic response of epitaxial iron-silicide nanoislands by controlled self-assembled growth, Phys. Rev. B. 96 (2017), doi:10.1103/PhysRevB.96.045415 045415.

[32] R V Pushkarev, N I Fainer, H Katsui, V V Kaichev, T Goto, Structural features and surface composition of epitaxial α-FeSi2 films obtained by CVD, Mater. Des. 137 (2018) 422–429, doi:10.1016/j.matdes.2017.10.030.

[33] A S Gouralnik, E V Pustovalov, K-W Lin, A L Chuvilin, S V Chusovitina, S A Dotsenko, A I Cherednichenko, V S Plotnikov, V A Ivanov, V I Belokon, I A Tkachenko, N G Galkin, An approach to growth of Fe–Si multilayers with controlled composition profile—a way to exchange coupled thin films, Nanotechnology. 28 (2017), doi:10.1088/1361-6528/aa5c96 115303.

[34] L Badía-Romano, J Rubín, C Magén, D E Bürgler, J Bartolomé, Iron silicide formation at different layers of (Fe/Si)3 multilayered structures determined by conversion electron Mössbauer spectroscopy, J. Appl. Phys. 116 (2014), doi:10.1063/1.4887522 023907.

[35] N Onda, H Sirringhaus, S Goncalves-Conto, C Schwarz, S Zehnder, H von Känel, Epitaxy of cubic iron silicides on Si(111), Appl. Surf. Sci. 73 (1993) 124–130, doi:10.1016/0169-4332(93)90155-5.

[36] A Hassani, A Makan, K Sbiaai, A Tabyaoui, A Hasnaoui, Incidence energy effect and impact assessment during homoepitaxial growth of nickel on (001), (111) and (110) surfaces, Thin Solid Films 640 (2017) 123–133, doi:10.1016/j.tsf.2017.09.006.

[37] Z-H Hong, S-F Hwang, T-H Fang, Atomic-level stress calculation and surface roughness of film deposition process using molecular dynamics simulation, Comput. Mater. Sci. 48 (2010) 520–528, doi:10.1016/j.commatsci.2010.02.018.

[38] A Hassani, A Makan, K Sbiaai, A Tabyaoui, A Hasnaoui, Molecular dynamics study of growth and interface structure during aluminum deposition on

[39] H El Azrak, A Hassani, F Eddiai, M Dardouri, M Monkade, A Arbaoui, K Sbiaai, A Hasnaoui, Investigation of fcc and hcp island nucleated during homoepitaxial growth of copper by molecular dynamics simulation, Superlattices Microstruct. 127 (2019) 118–122, doi:10.1016/j.spmi.2017.12.056.

[40] S Divi, A Chatterjee, Study of silicon thin film growth at high deposition rates using parallel replica molecular dynamics simulations, Energy Procedia 54 (2014) 270–280, doi:10.1016/j.egypro.2014.07.270.

[41] F V Grigoriev, V B Sulimov, A V Tikhonravov, Atomistic simulation of the glancing angle deposition of SiO2 thin films, J. Non-Cryst. Solids 512 (2019) 98–102, doi:10.1016/j.jnoncrysol.2019.02.016.

[42] Y Luo, M Lin, N Zhou, H Huang, C-T Tsai, L Zhou, Molecular dynamics simulation study of the microstructure of a-Si: H thin film grown by oblique-angle deposition, Phys. B 545 (2018) 80–85, doi:10.1016/j.physb.2018.05.042.

[43] G Zhu, J Sun, L Zhang, Z Gan, Molecular dynamics simulation of temperature effects on deposition of Cu film on Si by magnetron sputtering, J. Cryst. Growth 492 (2018) 60–66, doi:10.1016/j.jcrysgro.2018.04.002.

[44] L Xie, L An, Q Peng, Q Qin, Y Zhang, Sensitive five-fold local symmetry to kinetic energy of depositing atoms in Cu-Zr thin film growth, Materials (Basel). 11 (2018), doi:10.3390/ma11122548.

[45] L Xie, P Brault, J-M Bauchire, A-L Thomann, L Bedra, Molecular dynamics simulations of clusters and thin film growth in the context of plasma sputtering deposition, J. Phys. D: Appl. Phys. 47 (2014), doi:10.1088/0022-3727/47/22/224004 224004.

[46] A S Tarasov, A V Lukyanenko, I A Tarasov, I A Bondarev, T E Smolyarova, N N Kosyrev, V A Komarov, I A Yakovlev, M N Volochaev, L A Solovyov, A A Shemukhin, S N Varnakov, S G Ovchinnikov, G S Patrin, N V Volkov, Approach to form planar structures based on epitaxial Fe1−xSix films grown on Si(111), Thin Solid Films 642 (2017) 20–24, doi:10.1016/j.tsf.2017.09.025.

[47] I A Tarasov, M A Visotin, A S Aleksandrovsky, N N Kosyrev, I A Yakovlev, M S Molokeev, A V Lukyanenko, A S Krylov, A S Fedorov, S N Varnakov, S G Ovchinnikov, Si/Fe flux ratio influence on growth and physical properties of polycrystalline β-FeSi2 thin films on Si(100) surface, J. Magn. Magn. Mater. 440 (2017) 144–152, doi:10.1016/j.jmmm.2016.12.084.

[48] A S Tarasov, A V Lukyanenko, M V Rautskii, I A Bondarev, D A Smolyakov, I A Tarasov, I A Yakovlev, S N Varnakov, S G Ovchinnikov, F A Baron, N V Volkov, Spin-dependent electrical hole extraction from low doped p-Si via the interface states in a Fe3Si/p-Si structure, Semicond. Sci. Technol. 34 (2019), doi:10.1088/1361-6641/ab0327 035024.

[49] T D Nguyen, GPU-accelerated tersoff potentials for massively parallel molecular dynamics simulations, Comput. Phys. Commun. 212 (2017) 113–122, doi:10.1016/j.cpc.2016.10.020.

[50] S Plimpton, Fast parallel algorithms for short-range molecular dynamics, J. Comput. Phys. 117 (1995) 1–19, doi:10.1006/jcph.1995.1039.

[51] A Stukowski, Visualization and analysis of atomistic simulation data with OVITO–the open visualization tool, Modelling Simul. Mater. Sci. Eng. 18 (2009), doi:10.1088/0965-0393/18/1/015012 015012.

[52] S P Coleman, D E Spearot, L Capolungo, Virtual diffraction analysis of Ni [0hspace0.167em1hspace0.167em0] symmetric tilt grain boundaries, Modelling Simul. Mater. Sci. Eng. 21 (2013), doi:10.1088/0965-0393/21/5/055020 055020.

[53] H. Childs, VisIt: An End-User Tool for Visualizing and Analyzing Very Large Data, (2012). https://escholarship.org/uc/item/69r5m58v (accessed December 26, 2019).

[54] [1401.1310] Bond order potential for FeSi, (n.d.). https://arxiv.org/abs/1401.1310 (accessed December 26, 2019).

[55] P Erhart, K Albe, Analytical potential for atomistic simulations of silicon, carbon, and silicon carbide, Phys. Rev. B. 71 (2005), doi:10.1103/PhysRevB.71.035211 035211.

[56] M Müller, P Erhart, K Albe, Analytic bond-order potential for bcc and fcc iron—comparison with established embedded-atom method potentials, J. Phys.: Condens. Matter. 19 (2007) 326220, doi:10.1088/0953-8984/19/32/326220.

[57] P Hohenberg, W Kohn, Inhomogeneous electron gas, Phys. Rev. 136 (1964) B864–B871.

[58] W Kohn, L J Sham, Self-consistent equations including exchange and correlation effects, Phys. Rev. 140 (1965) A1133–A1138.

[59] G Kresse, J Furthmüller, Efficient iterative schemes for ab initio total-energy calculations using a plane-wave basis set, Phys. Rev. B. 54 (1996) 11169–11186.

[60] G Kresse, J Furthmüller, Efficiency of ab-initio total energy calculations for metals and semiconductors using a plane-wave basis set, Comput. Mater. Sci. 6 (1996) 15–50, doi:10.1016/0927-0256(96)00008-0.

[61] G Kresse, J Hafner, Ab initio molecular dynamics for liquid metals, Phys. Rev. B. 47 (1993) 558–561, doi:10.1103/PhysRevB.47.558.

[62] J P Perdew, K Burke, M Ernzerhof, Generalized gradient approximation made simple, Phys. Rev. Lett. 77 (1996) 3865–3868.

[63] Y Maeda, Y Kawakubo, Y Noguchi, K Narumi, S Sakai, Ion beam analysis of Heusler alloy Fe3Si epitaxially grown on Si(111), Phys. Status Solidi C 11 (2014) 1570–1573, doi:10.1002/pssc.201400027.

[64] S Dennler, J Hafner, First-principles study of lattice dynamics and diffusion in DO3-typeFe3Si, Phys. Rev. B. 73 (2006), doi:10.1103/PhysRevB.73.174303 174303.

[65] M N Volochaev, I A Tarasov, Y Y Loginov, A G Cherkov, I V Kovalev, The regularities of phase formation in Fe3Si(111)/Si(111) structure at vacuum annealing, J. Phys.: Conf. Ser. 857 (2017) 012053, doi:10.1088/1742-6596/857/1/012053.

Ni(100) substrate, Appl. Surf. Sci. 349 (2015) 785–791, doi:10.1016/j.apsusc.2015.05.076.

[66] R Nakane, S Sugahara, M Tanaka, Structural and magnetic properties of ferromagnetic Fe1−xSix (0.18 ≤ x ≤ 0.33) films formed by rapid thermal annealing on silicon-on-insulator substrates, J. Appl. Phys. 117 (2015), doi:10.1063/1.4915335.

[67] F Stromberg, S Bedanta, C Antoniak, W Keune, H Wende, FeSi diffusion barriers in Fe/FeSi/Si/FeSi/Fe multilayers and oscillatory antiferromagnetic exchange coupling, J. Phys.: Condens. Matter. 20 (2008), doi:10.1088/0953-8984/20/42/425205 425205.